

f^s	snow forces
f^{snow}	snow force
$(f^{snow})_{BO}$	snow force (Brown and Outwater model)
$(f^{snow})_{EF}$	snow force (elastic foundation model)
f_n^{snow}	snow force acting normal to the base of the snowboard
f_t^{snow}	snow force acting tangential to the base of the snowboard
$(GJ)'$	equivalent torsional stiffness
G	shear modulus
g	gravitational acceleration
h_{cg}	distance between the snowboard and the center of gravity (Z direction)
h_{cg}^0	neutral position of the center of gravity
H_{sb}	snowboarder height
K_{sn}	snow stiffness
k^{EI}, k^{GJ}, k^C	nodal spring stiffnesses
L	total length of snowboard
L_B	distance between the two boots along the $a-a$ line
L_r	running length
L_{tail}	length of snowboard from ACP to tail
L_{tip}	length of snowboard from FCP to tip
M_b^x, T_b^y, M_b^z	moments applied at the back boot
M_f^x, T_f^y, M_f^z	moments applied at the front boot
M_p^B, M_q^B, M_r^B	“midpoint” moments at point B in the path coordinate system
MRS	mid-running surface
\hat{M}_x	bending moment about the x axis
M_x, M_y, M_{xy}	in-plane moments
m	total mass of the snowboard
m_{sb}	mass of the snowboarder
N	number of points in the relevant data set
N_x, N_y	in-plane forces
nb	node just aft of the back boot
nf	node just forward of the front boot

n_α	number of points in the relevant data set that do not satisfy the safe turn requirement
n_{cg}	number of points in the relevant data set that do not satisfy allowable ranges of the center of gravity position of the snowboarder
n_s	number of points in the relevant data set that do not fall within the snowboarder's skill level ranges
<i>offset</i>	offset of centerline
$[P]$	the stiffness matrix for a beam element
P	force applied at <i>MRS</i> for flex calculation
$p - q - r$	coordinate system aligned with the course with origin at <i>B</i>
p_{cg}, q_{cg}, r_{cg}	location of the center of gravity in the $p - q - r$ coordinate system
R	radius of turn
R_1	radius of left turn
R_2	radius of right turn
\hat{r}_{ij}	position vector relating nodes <i>i</i> and <i>j</i>
S_E	total distance traveled from start to finish
S_M	distance traveled from start of course to the inflection point between the two turns
s	distance along path
SW	swingweight
\hat{T}	applied torque
T	transverse inertia force
T_A	torque applied at <i>ACP</i>
T_F	torque applied at <i>FCP</i>
T_p, T_q, T_r	components of the transverse inertia force in the path coordinate system
T^y	torque applied at each boot
$[T_{LG}]$	transformation matrices relating the $x - y - z$ and $p - q - r$ coordinate systems
$[T_p], [T_q], [T_r]$	transformation matrix relating the axes
$[T_{SG}]$	transformation matrices relating the $X - Y - Z$ and $p - q - r$ coordinate systems
$[T_X], [T_Y], [T_Z]$	transformation matrices describing rotation about the <i>X</i> , <i>Y</i> , and <i>Z</i> axes
t	snowboard thickness
t	time
t_c	core thickness

t^d	equilibrating torques
t^e	equilibrium torques
t_e	time to complete course
t^s	snow torques
u_{\max}	depth of the deepest edge in the snow
U	snow depth
v	speed
v_0	initial speed
v_{\max}	maximum allowable speed
v_{new}	velocity at the end of a segment of the turn
W	weight of the snowboarder
$[W]$	compliance matrix
W^b, W^f	weight of the snowboarder on the back and front boots
W_p, W_q, W_r	components of weight in the path coordinate system
W_{22}, W_{24}, W_{44}	elements of the compliance matrix
$X - Y - Z$	snowboard-fixed coordinate system with origin at B
$\tilde{X} - \tilde{Y} - \tilde{Z}$	snowboard based coordinate system with origin at MRS
$x - y - z$	local coordinate system with origin at the centroid of a segment
$\hat{x}^{ele}, \hat{y}^{ele}, \hat{z}^{ele}$	unit vectors describing the $x - y - z$ coordinate system for each element
$\hat{x}^{node}, \hat{y}^{node}, \hat{z}^{node}$	unit vectors describing the $x - y - z$ coordinate system for each node
\hat{x}^{avg}	vector describing the “average” x coordinate of the two boots
$\hat{x}_{nb}, \hat{x}_{nf-1}$	unit vectors describing the local x coordinate at each boot
$\bar{x} - \bar{y} - \bar{z}$	local coordinate system with origin at the midpoint of the base
x_c	centroid location in the x direction
X_{cg}, Y_{cg}	location of the center of gravity
z_c	centroid location in the z direction

Greek Letters

α, β, δ	components of the inverse of the $A-B-D$ matrix
α	yaw angle
β	roll angle

δdepth of the snowboard at point B
Δvertical deflection at <i>MRS</i> in flex calculation
$\Delta\alpha, \Delta\beta$allowable ranges of the yaw and roll for a given snowboarder
Δh_{cg}change in the center of gravity position
$(\Delta h_{cg})_h, (\Delta h_{cg})_{h+a}$change in the center of gravity position based on height and ability
Δslength of a segment of the path
Δttime required to travel one segment of the path
δposition of point <i>B</i> relative to the surface of the snow
ϕrotation angle
γ^ttwist angle
ηpitch angle
λoffset angle
κ_{cg}, ζ_{cg}position ranges of the center of gravity
ρdensity
ρ_aair density
$\frac{1}{\rho_x}$curvature of the longitudinal <i>y</i> axis passing through the centroid about the <i>x</i> axis
θ^ttotal bending angle
θ^bbending angle
θ^ccamber angle
ϑrate of twist
νPoisson's ratio
$\Omega_{0A}, \Omega_{AB}, \Omega_{BM}, \Omega_{MC}, \Omega_{CE}$	arc lengths for segments of the course
σ_fsnow force per unit area
Ξdisplacement of point <i>B</i> from undeformed position
Ψangle of twist
Ψ_Aangle of twist at <i>ACP</i>
Ψ_Fangle of twist at <i>FCP</i>
$\xi_{0B}, \xi_{BC}, \xi_{CE}$hill angle

Chapter 1

Introduction

The popularity of snowboarding has been increasing steadily since snowboards were first introduced in the early 1970's. To meet the needs of snowboarders with different abilities, manufacturers have introduced a variety of different snowboard designs. To this end, manufacturers use different materials and different shapes. The challenge facing the snowboard designer is to select the proper combination of materials and shape that result in the desired performance. Currently, most manufacturers rely on a trial and error procedure in designing snowboards. In this process prototypes are built and their mechanical properties such as the bending and torsional stiffnesses, flex, twist, natural frequencies and damping are measured in the laboratory. The laboratory tests are followed by on-snow test runs after which the rider gives a qualitative review. A more quantitative evaluation of the on-snow behavior of snowboards was described by Sutton [1], who collected strain gauge and accelerometer data with the rider executing turns and jumps. These data provided information on axial and torsional bending, natural frequency, and damping. While the results of these laboratory and on-snow measurements provide some indication of the suitability of the snowboard, they do not lead directly to snowboard designs best suited for specified snowboarders under specified snow and course conditions.

The design can be greatly facilitated by a process based on fundamental engineering principles. Although such an approach has yet to be applied to snowboards, it has been applied to alpine skis (see Nordt et al. [2, 3] and the references cited therein). Here, we follow the approach of Nordt et al. and develop models that provide the mechanical characteristics of snowboards and simulate the on-snow performance.

Chapter 2

Problem Statement

We consider a snowboard with a prescribed geometry and construction. The geometry is specified by the length, width, thickness, camber, and offset (Figure 2.1). The offset is the distance between the line passing through the centroid of each cross section (referred to as the centerline) and the line $a - a$ passing through the centers of the boots. The construction is specified by the properties, locations, and shapes of the components. Here, we consider snowboards with sandwich construction (Figure 2.2). The core may be wood, foam, or honeycomb. There is a composite laminate on each side of the core; these laminates may be comprised of plies reinforced by continuous or short fibers, fabric, or a combination of these. There is a top and a bottom layer usually made of polymeric materials such as ABS for the topsheet and polyethylene for the base. Narrow strips may be inserted to provide reinforcement and damping. There are two steel edges inserted in the base. Neither the cross section nor the shape of the snowboard need be symmetric.

Our objective is to model both the mechanical characteristics and the on-snow performance of the snowboard. The mechanical characteristics studied are the bending and torsional stiffnesses and the deflections under bending (flex) and torsion (twist). The on-snow performance characteristic of interest is the time required for a snowboarder to negotiate safely a prescribed course. Specifically, we consider a snowboarder of given height, weight, weight distribution (Figure 2.3), and skill level entering an S-shaped course with speed v_0 . The course consists of two turns of radii R_1 and R_2 , with a total length of $R_1\Omega_1 + R_2\Omega_2$ (Figure 2.4). The slope need not be constant, but may vary along

the course from start O to finish E . The snow is smooth and its consistency is constant along the course. The snowboarder's skill level is specified by the maximum distances the center of gravity may move 'up and down', 'forward and backward', and 'sideways' (Figure 2.5), the allowable roll β and yaw α angles (Figure 2.6), and the maximum speed that the snowboarder can safely maintain throughout the course. There is an additional constraint imposed during the run to ensure that the turn can be executed safely with ease. To this end, it is required that the inside edge points 'inward', i.e. the tangent to the edge at every point in contact with the snow must point to the left for a left turn and to the right for a right turn (Figure 2.7).

The objective is to develop a model that provides the time required for the snowboarder to complete the course such that he stays within his skill level ranges and maintains the proper snowboard orientation. The time t_e required to complete the turn is taken as an indication of the snowboard's performance with a faster board being preferable to a slower one.

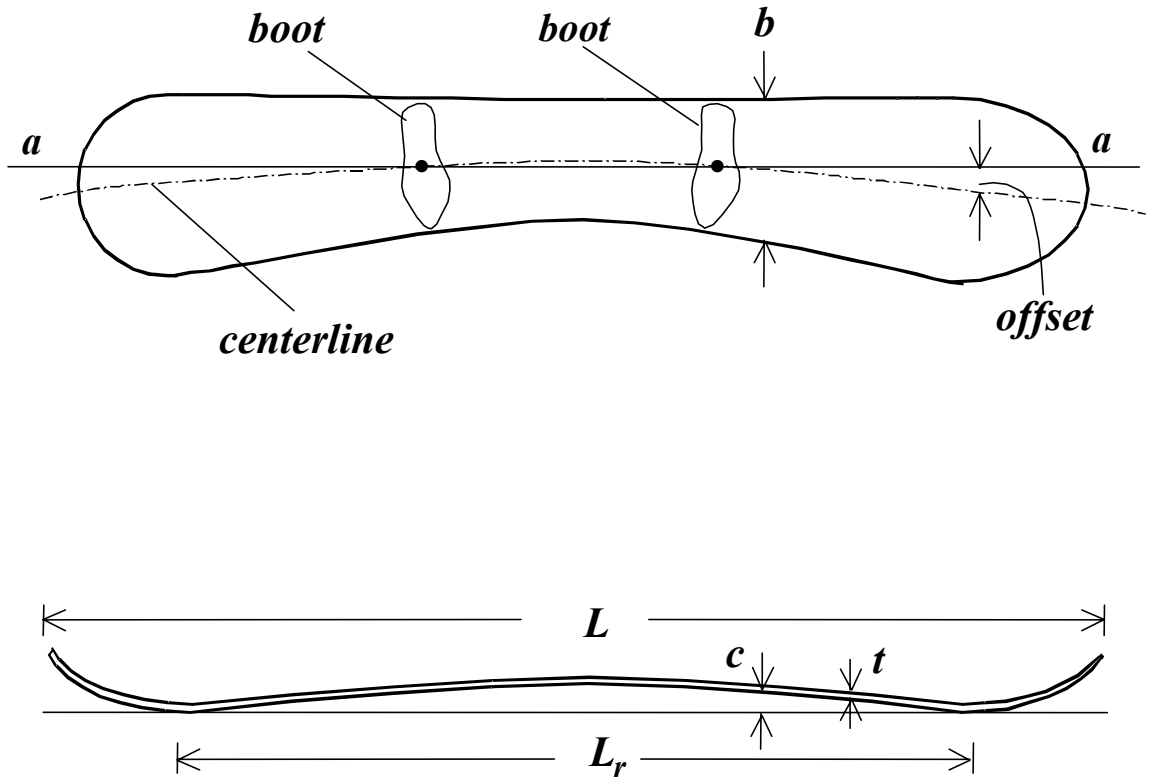


Figure 2.1: Snowboard geometry with length L , running length L_r , width b , thickness t , camber c , and offset. The centerline passes through the centroid of each cross section (see Appendix B).

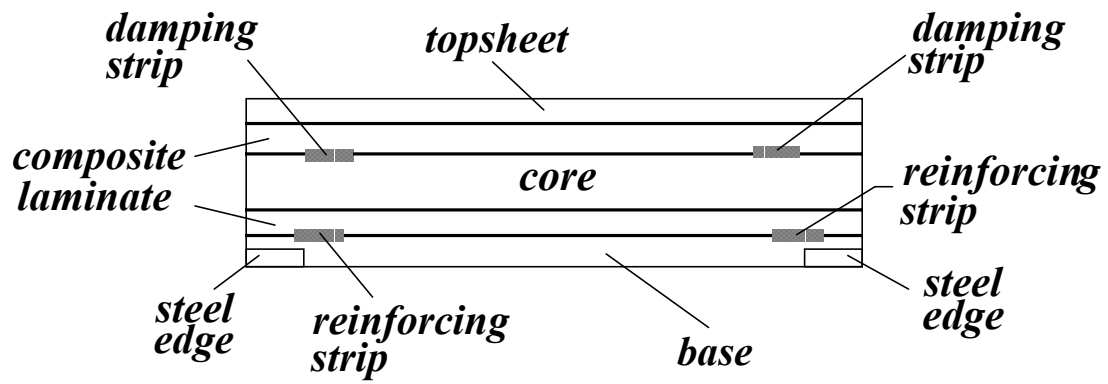


Figure 2.2: Snowboard construction.

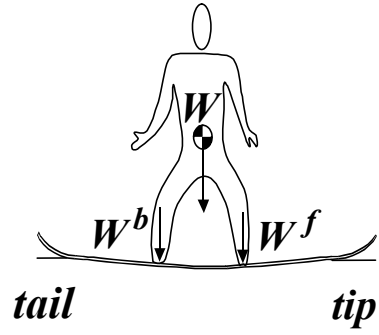


Figure 2.3: The weight distribution of the snowboarder; W is the weight of the snowboarder, and W^f and W^b represent the weights on the front and back boots.

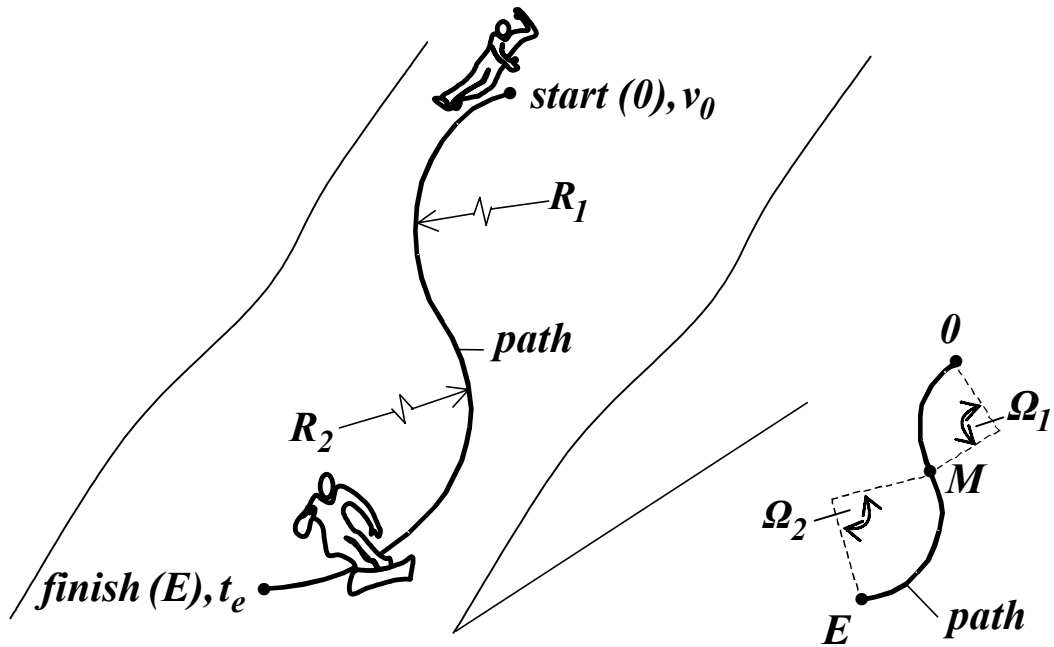


Figure 2.4: Description of the course; R_1 and R_2 are the radii of the two linked turns, and $R_1\Omega_1 + R_2\Omega_2$ is the length of the path. The snowboarder enters with speed v_0 , and t_e is the time required to complete the course.

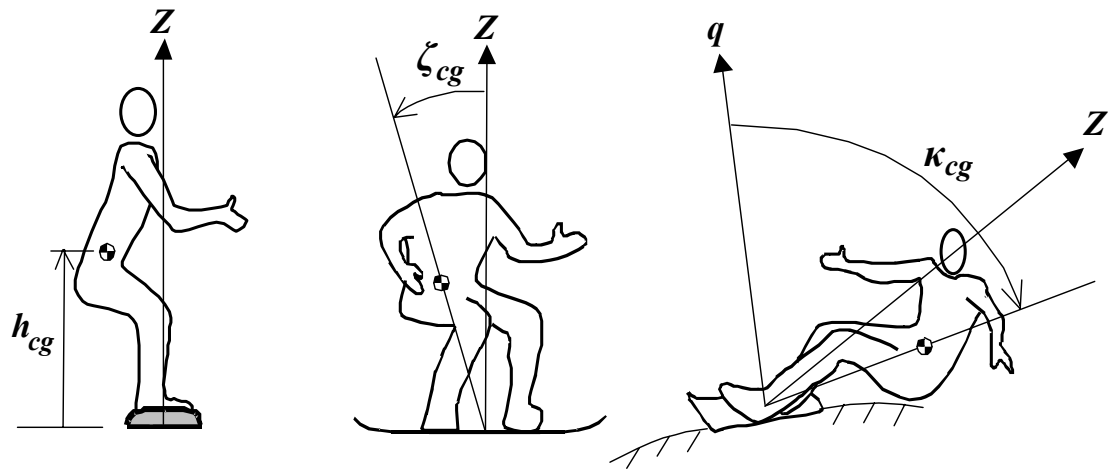


Figure 2.5: The motion of the center of gravity ‘up and down’ (left), ‘forward and back’ with respect to the normal Z to the snowboard (middle), and ‘sideways’ with respect to the normal q to the slope (right).

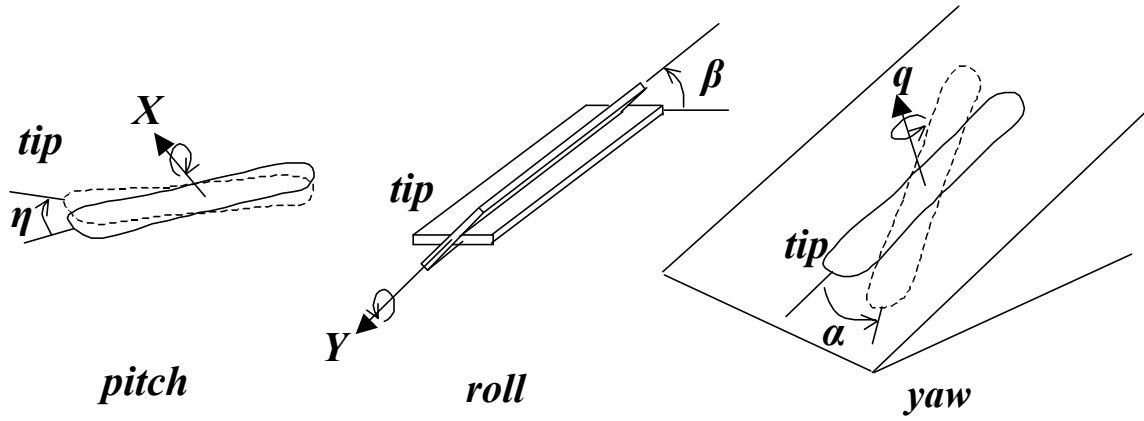


Figure 2.6: Illustration of the pitch, roll, and yaw. Pitch and roll are about the snowboard's transverse X and longitudinal Y axes respectively, and yaw is about the q axis perpendicular to the snow. The X , Y , and q coordinates are defined in Appendix A.

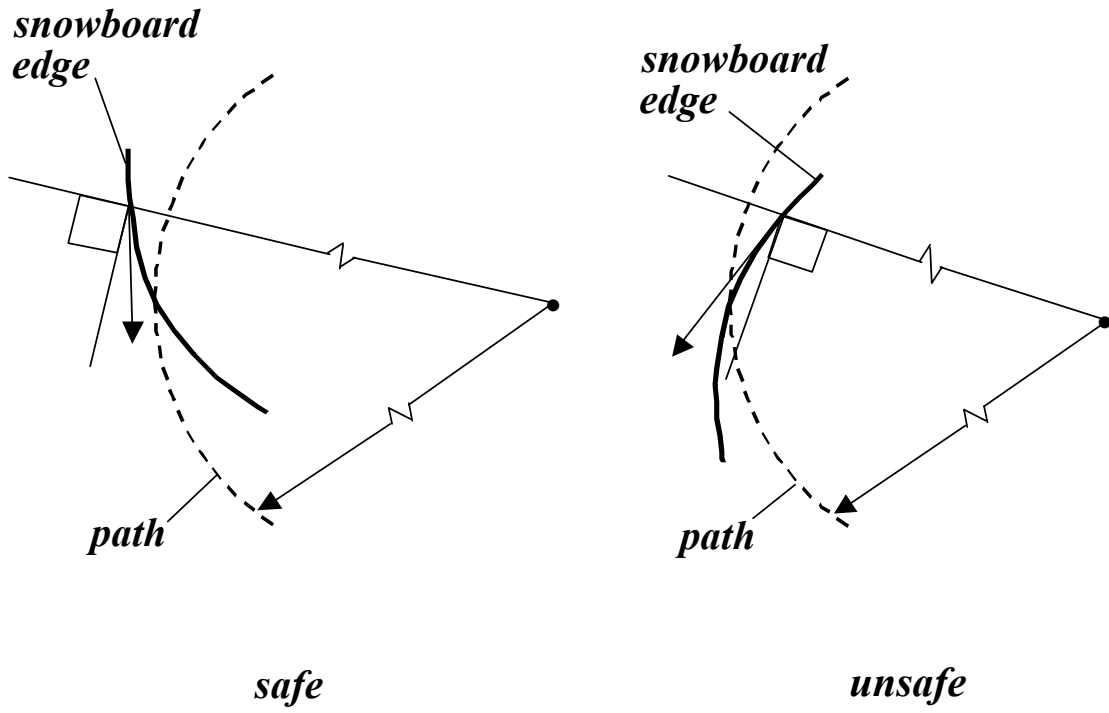


Figure 2.7: Condition for executing a safe turn with ease.

Chapter 3

Bending and Torsion

We treat the snowboard as a thin beam and relate the applied moment and applied torque to the radius of curvature and the rate of twist by the relationship [4, page 209]

$$\begin{Bmatrix} \frac{1}{\rho_x} \\ \mathfrak{G} \end{Bmatrix} = \begin{bmatrix} W_{22} & W_{24} \\ W_{24} & W_{44} \end{bmatrix} \begin{Bmatrix} \hat{M}_x \\ \hat{T} \end{Bmatrix} \quad (3.1)$$

where \hat{M}_x is the bending moment about the x axis, $\frac{1}{\rho_x}$ is the curvature of the longitudinal y axis (Figure 3.1), \hat{T} is the applied torque, \mathfrak{G} is the rate of twist which is related to the angle of twist ψ by the expression $\mathfrak{G} = \frac{\partial \psi}{\partial y}$ (Figure 3.2), and W_{22} , W_{24} , and W_{44} are the elements of the compliance matrix (Appendix C). The origin of the $x - y - z$ coordinate system is at the centroid.

When only a bending moment is applied we have

$$\frac{1}{\rho_x} = W_{22}\hat{M}_x \quad \mathfrak{G} = W_{24}\hat{M}_x \quad (3.2)$$

This equation shows that when only a bending moment is applied, $\frac{1}{W_{22}}$ is the equivalent bending stiffness $(EI)'$

$$(EI)' = \frac{\hat{M}_x}{\frac{1}{\rho_x}} = \frac{1}{W_{22}} \quad (3.3)$$

When only a torque is applied we have

$$\frac{1}{\rho_x} = W_{24}\hat{T} \quad \mathfrak{G} = W_{44}\hat{T} \quad (3.4)$$

The ratio $\frac{1}{W_{44}}$ is the equivalent torsional stiffness $(GJ)'$

$$(GJ)' = \frac{\hat{T}}{\theta} = \frac{1}{W_{44}} \quad (3.5)$$

When W_{24} is non-zero there is a bend-twist coupling such that a bending moment causes twist and a torque causes deflection (Figure 3.3).

The flex is a measure of the flexural stiffness of the snowboard. To determine the flex the snowboard is subjected to three-point bending as shown in Figure 3.4. The flex is

$$\text{Flex} = \frac{P}{\Delta} \quad (3.6)$$

where P is the applied load and Δ is the deflection at the point where the load is applied.

The forebody and aftbody twists are measures of the torsional stiffness of the snowboard. To determine the forebody and aftbody twists of the snowboard we consider a snowboard clamped at the mid-running surface *MRS* (Figure 3.4). The forebody and aftbody twists (Figure 3.5) are defined as

$$\text{forebody twist} = \frac{\hat{T}_F}{\psi_F} \quad \text{aftbody twist} = \frac{\hat{T}_A}{\psi_A} \quad (3.7)$$

The parameters \hat{T}_F and \hat{T}_A represent the torques applied at the forward *FCP* and aft *ACP* contact points, and ψ_F and ψ_A are the corresponding angles of twist.

The flex and twist are calculated by a finite element method using beam elements [5]. The stiffness matrix $[P]$ of the beam used in these calculations is

$$[P] = \begin{bmatrix} W_{22} & W_{24} \\ W_{24} & W_{44} \end{bmatrix}^{-1} \quad (3.8)$$

3.1 Computer Code “Snowboard-MECH”

A computer code designated as Snowboard-MECH was written for calculating the mechanical characteristics. The input parameters are the geometry, material properties,

and the construction (layup) of the cross section. The output includes the bending stiffness along the length, the torsional stiffness along the length, the flex, and the forebody and aftbody twists (Table 3.1).

3.2 Validation – Mechanical Characteristics

To assess the accuracies of the models, mechanical characteristics calculated by these models were compared to analytical results obtained for three “snowboard-like” structures (Figure 3.6) and to data obtained for two actual snowboards (Figure 3.7):

1. flat aluminum beam of constant cross section
2. flat steel box beam of constant cross section
3. flat aluminum-wood-aluminum sandwich beam of constant cross section
4. K2 Astar 147
5. K2 Spitfire 164

The mechanical characteristics of the three snowboard-like structures and the two snowboards were calculated by the models. The mechanical characteristics of the three snowboard-like structures were also calculated analytically using the formulas given in Roark [6]. The dimensions and material properties used in the calculations are listed in Tables 3.2 and 3.3. The mechanical characteristics of the K2 Astar 147 and the K2 Spitfire 164 were measured by the author at K2 Corporation.

For the three snowboard-like structures illustrated in Figure 3.6 the bending stiffness, flex, torsional stiffness, fore and aftbody twists calculated analytically and by the present models agree within 0.1 percent. For the K2 Astar 147 and the K2 Spitfire 164 snowboards the measured bending stiffness, flex, forebody and aftbody twists are compared to values calculated by the models. The results, presented in Figures 3.8-3.10, show good agreement between the measured and the calculated mechanical characteristic values.

The aforementioned results suggest that the models would be useful tools for determining the mechanical characteristics of snowboards.

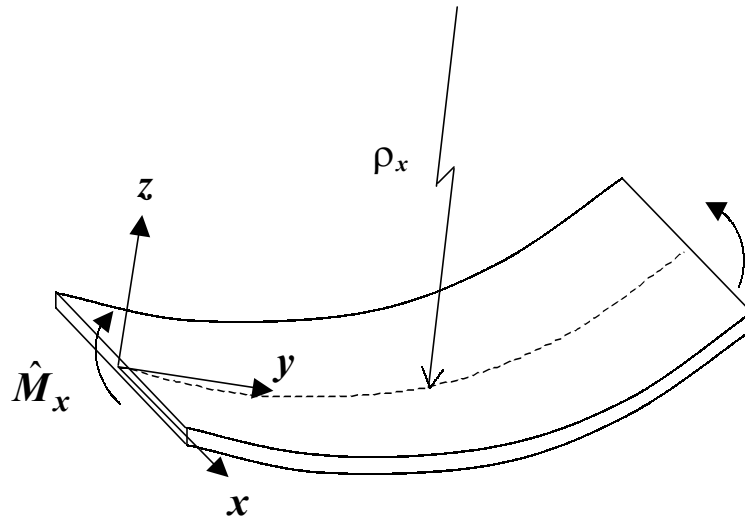


Figure 3.1: The bending moment and the curvature.

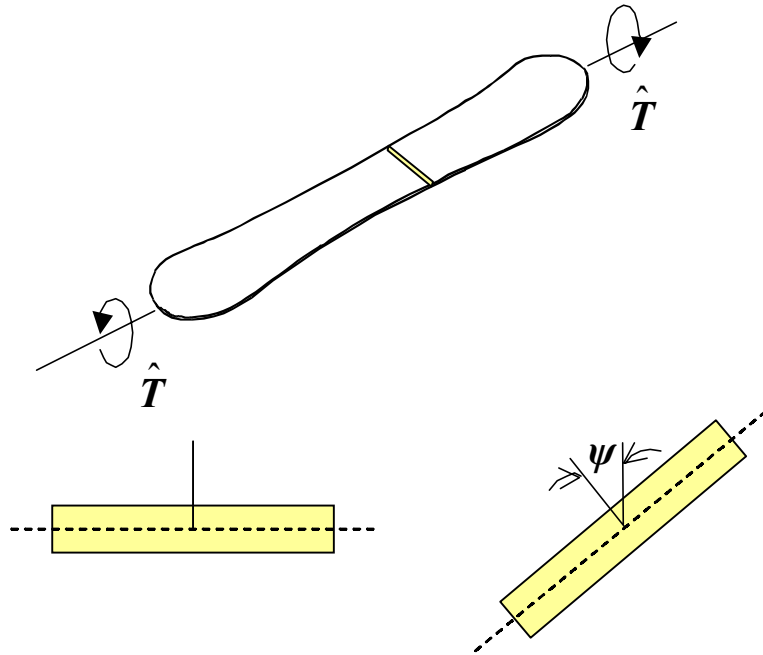


Figure 3.2: Torque applied to the snowboard and the angle of twist.

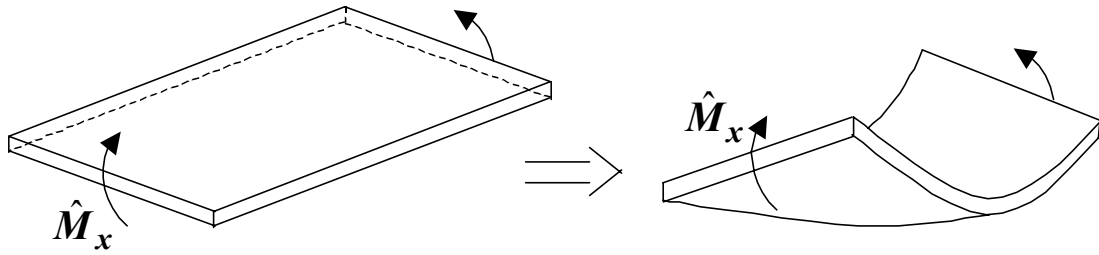


Figure 3.3: The bend-twist coupling of a snowboard with unsymmetrical construction subjected to a bending moment.

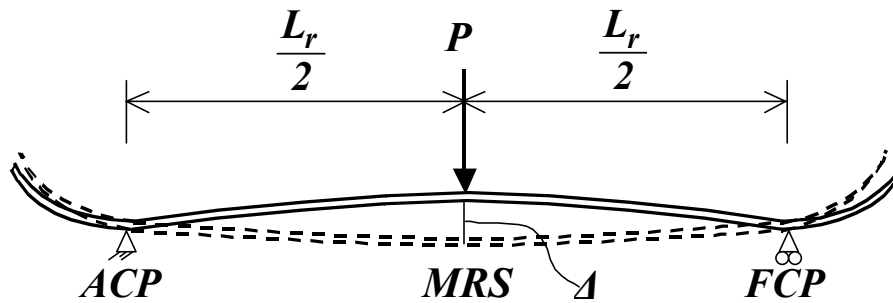


Figure 3.4: Snowboard in 3 point bending. MRS is the mid-running surface, FCP and ACP are the forward and aft contact points. The flex is: $\text{Flex} = \frac{P}{\Delta}$.

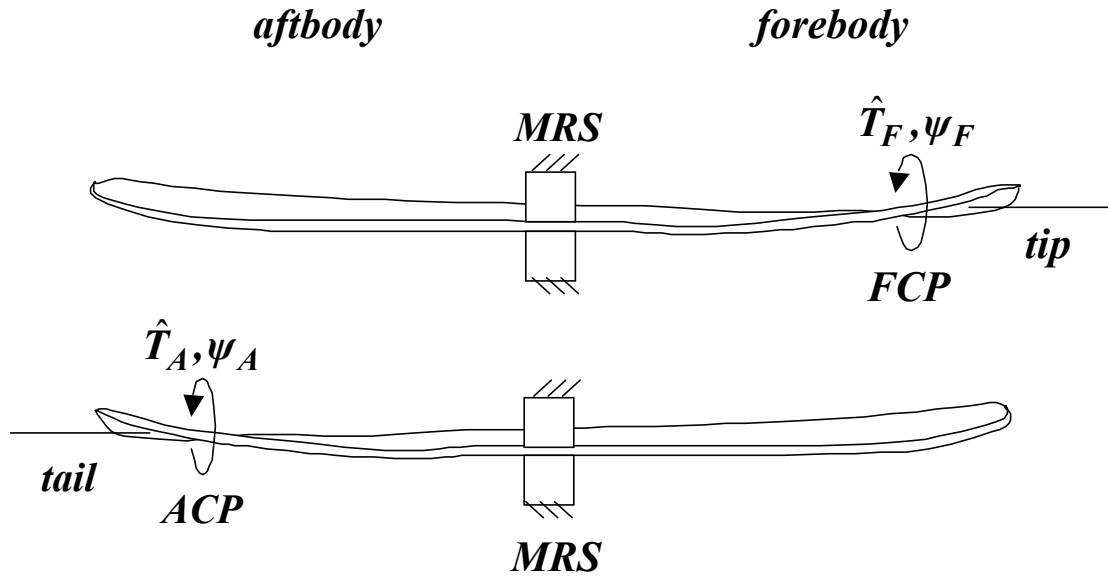


Figure 3.5: Forebody and aftbody twists.

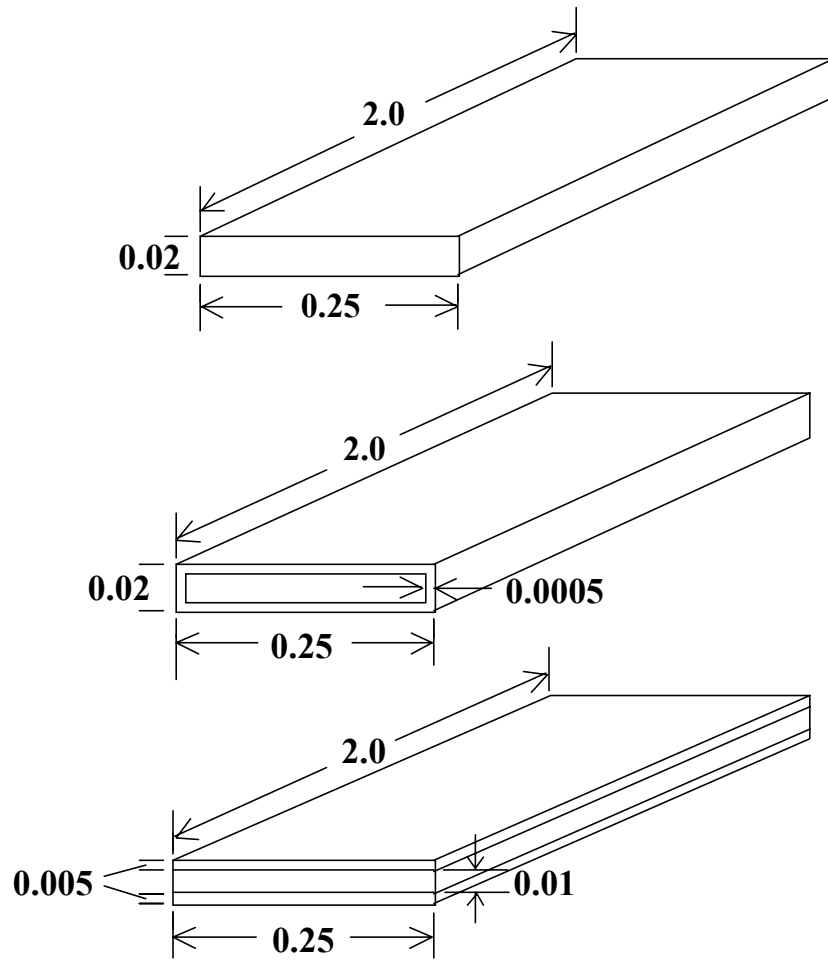


Figure 3.6: Dimensions of the solid aluminum beam, the steel box beam, and the aluminum-wood-aluminum sandwich beam used in analysis. All dimensions are in meters.

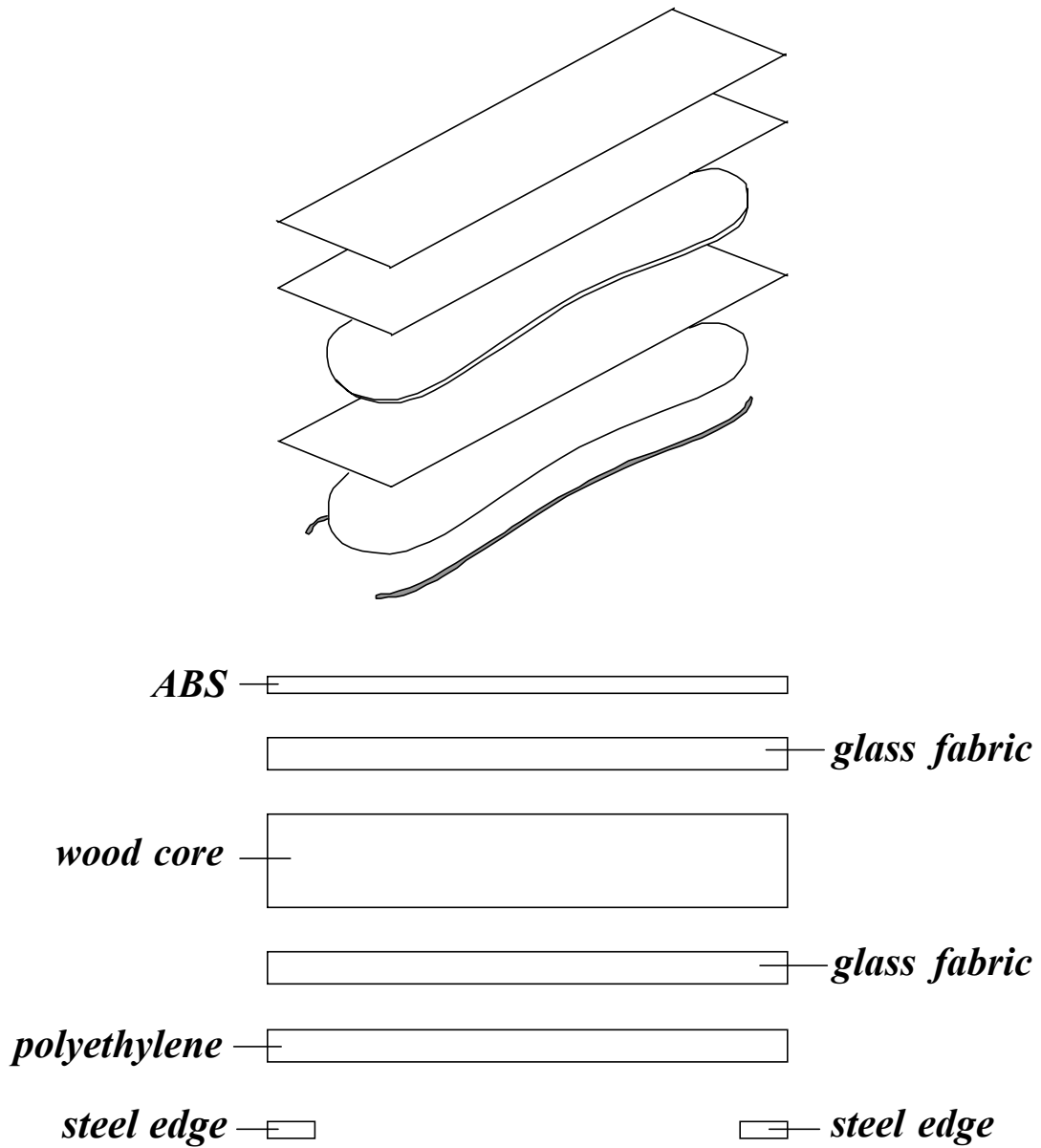


Figure 3.7: The layup of the K2 Astar 147 and the K2 Spitfire 164 snowboards. The top layer is 22 oz glass fabric for the Astar and 25 oz glass fabric for the Spitfire. The bottom layer is 22 oz glass fabric for both snowboards. The dimensions are given in Tables 3.1-3.3.

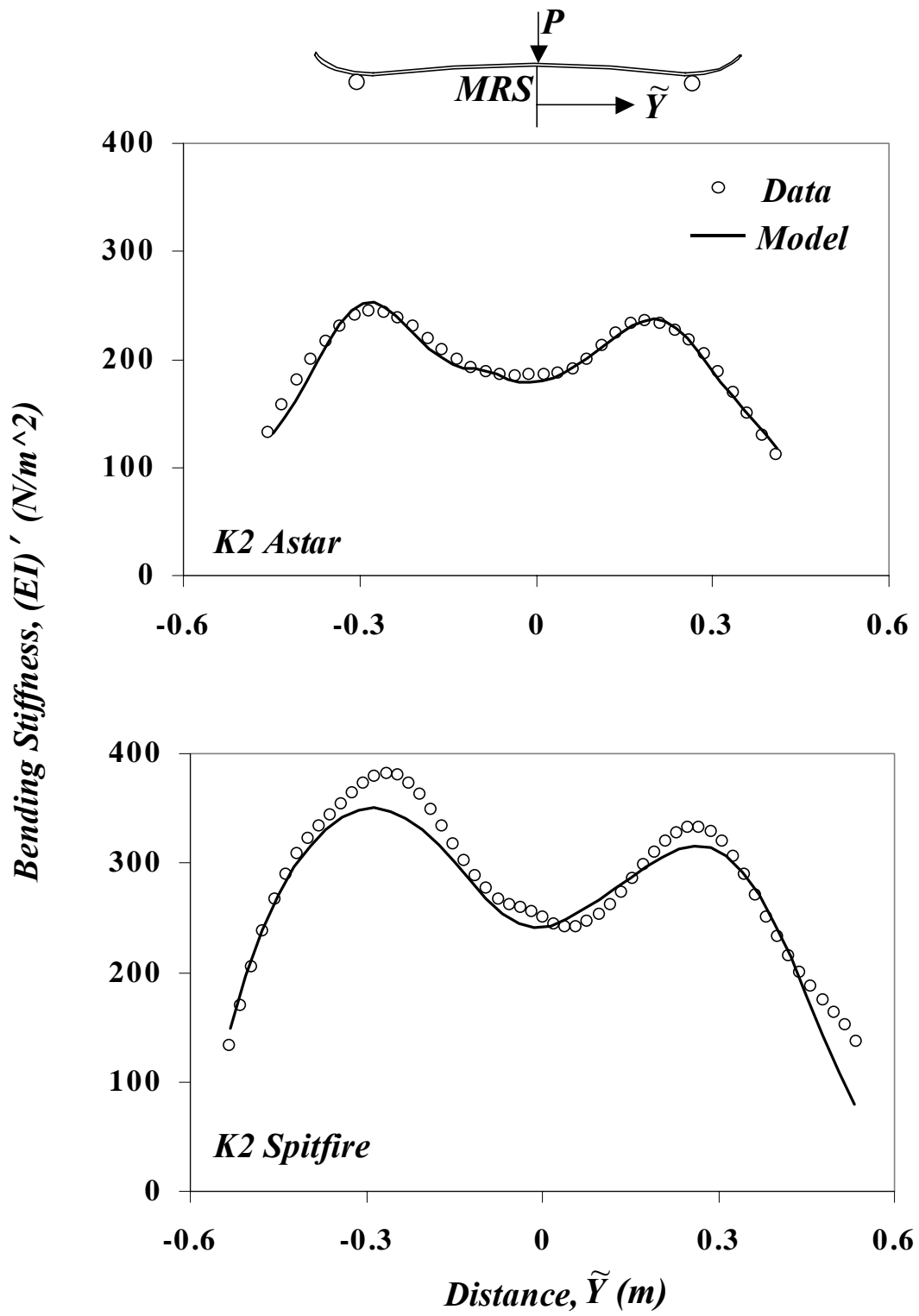


Figure 3.8: Bending stiffnesses of the K2 snowboards.

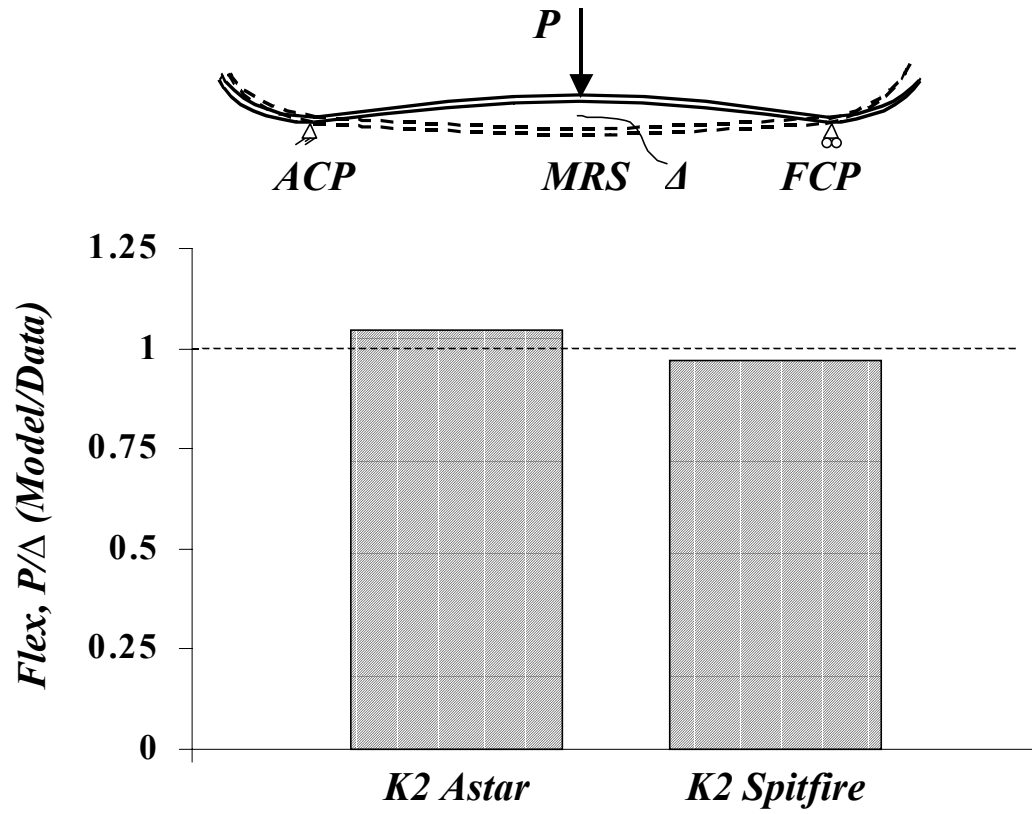


Figure 3.9: Flex calculated by the model compared to data.

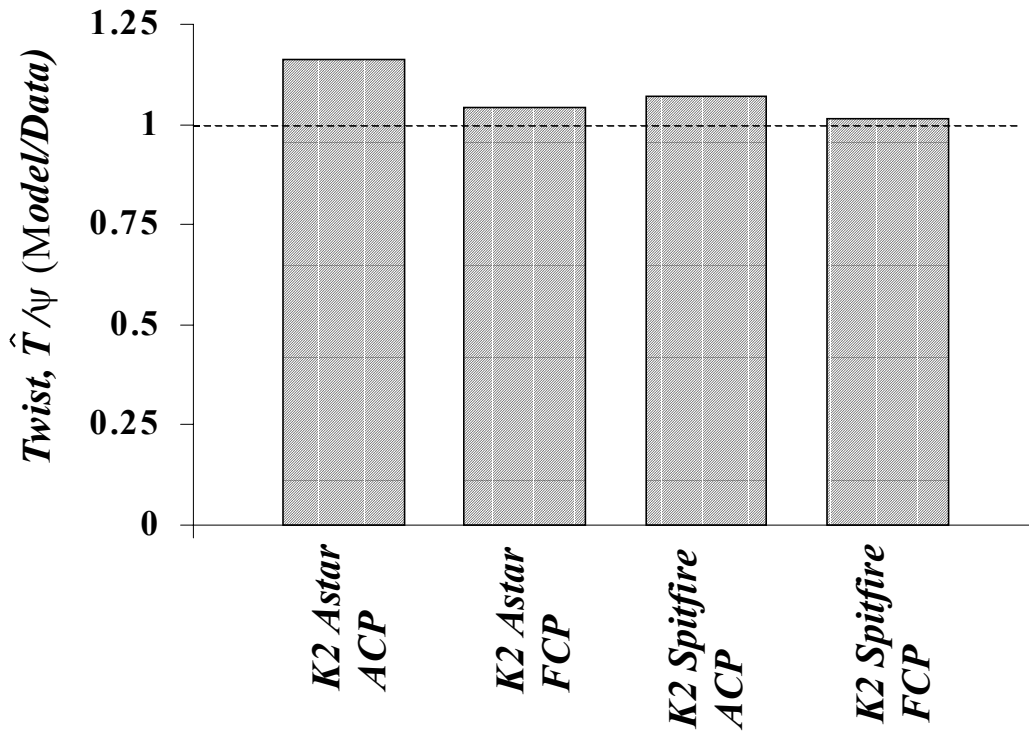


Figure 3.10: Twist calculated by the model compared to data. *FCP* and *ACP* indicate forebody and aftbody twist.

Input

Snowboard

- Geometry (Figure 2.1)
- Material properties (see Table 3.3)
- Layup (Figure 3.7)

Output

Bending stiffness along the length

Torsional stiffness along the length

Flex

Forebody twist

Aftbody twist

Table 3.1: Input and output of the computer code “Snowboard-MECH”